from the Ministry of Education, Culture, Sports, Science and Technology of Japan; Takeo Suzuki, Grant-in-Aid for Scientific Research from the Ministry of Education, Culture, Sports, Science and Technology of Japan; K. Tomizawa, the Japan Society for the Promotion of Science (JSPS) through its "Funding Program for Next Generation World-Leading Researchers," and the Takeda Science Foundation.
Expert Testimony: None declared.
Patents: None declared.
Role of Sponsor: The funding organizations played no role in the design of study, choice of enrolled patients, review and interpretation of data, or preparation or approval of manuscript.
Acknowledgments: We thank N. Maeda, S. Watanabe, and N. Takahashi for technical assistance.

References

1. Gustilo EM, Vendeix FA, Agris PF. tRNA's modifications bring order to gene expression. Curr Opin Microbiol 2008;11:134–40.
2. Motorin Y, Helm M. RNA stabilization by modified nucleotides. Biochemistry 2010;49:4934–44.
3. Suzuki T. Biosynthesis and function of tRNA wobble modifications. In: Grosjean H, ed. Topics in current genetics. Vol. 12. Fine-tuning of RNA functions by modification and editing. Berlin: Springer-Verlag; 2005. p 23–69.
4. Wei FY, Suzuki T, Watanabe S, Kimura S, Kaitsuka T, Fujimura A, et al. Deficit of tRNA(Lys) modification by Cdkal1 causes the development of type 2 diabetes in mice. J Clin Invest 2011;121:3598–608.
5. Yasukawa T, Suzuki T, Ishii N, Ohta S, Watanabe K. Wobble modification defect in tRNA disturbs codon–anticodon interaction in a mitochondrial disease. EMBO J 2001;20:4794–802.
6. Kirino Y, Goto Y, Campos Y, Arenas J, Suzuki T. Specific correlation between the wobble modification deficiency in mutant tRNAs and the clinical features of a human mitochondrial disease. Proc Natl Acad Sci U S A 2005;102:7127–32.
7. Steinthorsdottir V, Thorleifsson G, Reynisdottir I, Benediktsson R, Jonsdottir T, Walters GB, et al. A variant in CDKAL1 influences insulin response and risk of type 2 diabetes. Nat Genet 2007;39:770–5.
8. Diabetes Genetics Initiative of Broad Institute of Harvard and MIT, Lund University, and Novartis Institutes of BioMedical Research, Saxena R, Voight BF, Lyssenko V, et al. Genome-wide association analysis identifies loci for type 2 diabetes and triglyceride levels. Science 2007;316:1331–6.
9. Arragain S, Handelman SK, Forouhar F, Wei FY, Tomizawa K, Hunt JF, et al. Identification of eukaryotic and prokaryotic methylthiotransferase for biosynthesis of 2-methylthio-N^6-threonylcarbamoyladenosine in tRNA. J Biol Chem 2010;285:28425–33.
10. Suzuki T, Ikeuchi Y, Noma A, Suzuki T, Sakaguchi Y. Mass spectrometric identification and characterization of RNA-modifying enzymes. Methods Enzymol 2007;425:211–29.
11. Miyauchi K, Ohara T, Suzuki T. Automated parallel isolation of multiple species of non-coding RNAs by the reciprocal circulating chromatography method. Nucleic Acids Res 2007;35:e24.
12. Jühling F, Mörl M, Hartmann RK, Sprinzl M, Stadler PF, Pütz J. tRNAdb 2009: compilation of tRNA sequences and tRNA genes. Nucleic Acids Res 2009;37:D159–62.
13. Maden BE, Corbett ME, Heeney PA, Pugh K, Ajuh PM. Classical and novel approaches to the detection and localization of the numerous modified nucleotides in eukaryotic ribosomal RNA. Biochimie 1995;77:22–9.
14. Grosjean H, Motorin Y, Morin A. RNA-modifying and RNA-editing enzymes: methods for their detection. In: Grosjean H, Beene R, eds. Modification and editing of RNA. Washington, DC: ASM Press; 1998. p 21–46.
15. Chujo T, Suzuki T. Trmt61B is a methyltransferase responsible for 1-methyladenosine at position 58 of human mitochondrial tRNAs. RNA 2012;18:2269–76.
16. D'Silva S, Haider SJ, Phizicky EM. A domain of the actin binding protein Abp140 is the yeast methyltransferase responsible for 3-methylcytidine modification in the tRNA anti-codon loop. RNA 2011;17:1100–10.
17. Jenner LB, Demeshkina N, Yusupova G, Yusupov M. Structural aspects of messenger RNA reading frame maintenance by the ribosome. Nat Struct Mol Biol 2010;17:555–60.
18. Bondi A. van der Waals volumes and radii. J Phys Chem 1964;68:441–51.
19. Fukui T, Ikehara M. Polynuleotides XLVII. Synthesis and properties of poly(2-methylthio- and 2-ethylthioadenylic acid). Formation of non-Watson-Crick type complexes. Biochim Biophys Acta 1979;562:527–33.
20. Hokoshima T, Fukui T, Ikehara M, Tomita K. Molecular structure of a double helix that has non-Watson-Crick type base pairing formed by 2-substituted poly(A) and poly(U). Proc Natl Acad Sci U S A 1981;78:7309–13.
21. Moore AF, Jablonski KA, McAteer JB, Saxena R, Pollin TI, Franks PW, et al., and for the Diabetes Prevention Program Research Group. Extension of type 2 diabetes genome-wide association scan results in the Diabetes Prevention Program. Diabetes 2008;57:2503–10.
22. Okada Y, Kubo M, Ohmiya H, Takahashi A, Kumasaka N, Hosono N, et al. Common variants at CDKAL1 and KLF9 are associated with body mass index in East Asian populations. Nat Genet 2012;44:302–6.
23. Wen W, Cho YS, Zheng W, Dorajoo R, Kato N, Qi L, et al. Meta-analysis identifies common variants associated with body mass index in East Asians. Nat Genet 2012;44:307–11.
24. Barrett JC, Hansoul S, Nicolae DL, Cho JH, Duerr RH, Rioux JD, et al. Genome-wide association defines more than 30 distinct susceptibility loci for Crohn's disease. Nat Genet 2008;40:955–62.

Efficient Transduction of 11 Poly-arginine Peptide in an Ischemic Lesion of Mouse Brain

Yuki Gotanda,* Fan-Yan Wei,† Hideki Harada,* Keisuke Ohta,‡ Kei-ichiro Nakamura,‡ Kazuhito Tomizawa,† and Kazuo Ushijima*

Direct intracellular delivery of intact proteins has been successfully achieved by tagging cell-penetrating peptide (CPP), which consists of short positively charged amino acids, such as 11 poly-arginine (11R); however, in vivo delivery of the proteins to the brain has remained challenging because it is unclear whether CPP would enable proteins to cross the blood–brain barrier (BBB). In this study, we conducted an in vivo kinetic study to investigate the efficiency of 11R-mediated peptide delivery in the normal and ischemic brain. The 11R was observed in the microvessels and neurons surrounding the microvessels throughout the brain 1 hour after systemic administration, but the signal of the peptide was faint after 2 hours. In a transient middle cerebral artery occlusion mouse model, 11R was markedly enhanced and remained detectable in the cells on the ipsilateral side for as long as 8 hours after administration compared with the contralateral side. These results suggest that 11R is capable of in vivo delivery to the brain by passing through the BBB. Furthermore, 11R-mediated protein transduction could be used for the delivery of therapeutic molecules in cerebral ischemia. **Key Words:** Protein transduction—poly-arginine—brain—ischemia.

Introduction

Stroke is a leading cause of death and the principal cause of adult disability worldwide.[1] To treat an ischemic stroke, current therapies use thrombolytic approaches to dissolve blood clots.[2] These treatments restore blood flow and prevent further brain damage; however, there is no medicine that can treat brain damage and prevent neuronal cell death by directly targeting neuronal cells. One reason is the difficulty of crossing the blood–brain barrier (BBB), which is composed of a layer of specialized endothelial cells that segregate the brain from the circulating blood.[3] Extensive efforts have been made to engineer and deliver biologically active molecules to the brain across the BBB.[4]

Among the delivery systems, a technology using cell-penetrating peptide (CPP) has been emerging as a potential tool to pass through biological membranes.[5-7] CPP consists of short peptides containing positively charged amino acids, such as lysine and arginine. Protein transduction domains (PTDs) in the transactivator of transcription (TAT) protein of HIV and VP22 in herpes simplex virus 1 enable efficient intracellular transduction of peptides and proteins through a macropinocytosis-dependent mechanism.[8] Subsequent studies have aimed to apply TAT-derived PTD for in vivo delivery across the BBB, and it has been found that TAT-derived PTD is capable of transduction into the intact brain[9,10]; however, several groups have reported that TAT protein could not enter the intact brain using the same construct.[11,12] Currently, whether TAT-derived PTD is capable of

From the *Department of Anesthesiology, Kurume University School of Medicine, Fukuoka; †Department of Molecular Physiology, Faculty of Life Sciences, Kumamoto University, Kumamoto; and ‡Division of Microscopic and Developmental Anatomy, Department of Anatomy, Kurume University School of Medicine, Fukuoka, Japan.

Received September 10, 2013; revision received February 8, 2014; accepted February 26, 2014.

Address correspondence to Kazuhito Tomizawa, Department of Anesthesiology, Kurume University School of Medicine, Fukuoka, Japan. E-mail: tomikt@kumamoto-u.ac.jp.

1052-3057/$ - see front matter

http://dx.doi.org/10.1016/j.jstrokecerebrovasdis.2014.02.027

transduction to the intact brain is still controversial, and improvement of the delivery system is required to achieve high efficiency. We previously reported that 11 poly-arginine (11R) was capable of intracellular delivery both in vitro and in vivo, such as to the mouse kidney and heart, more efficiently than TAT.[13] Taken together, these studies suggest that 11R may be used as a potential tool to deliver biologically active molecules to the brain across the BBB.

In this study, we investigated whether 11R could enter intact and ischemic brains across the BBB after systemic administration.

Materials and Methods

Peptide Synthesis

Eleven arginine peptides (11R) composed of basic amino acids were chemically synthesized by Fmoc (9-fluorenylmethyloxycarbonyl) solid-phase peptide synthesis on Rink amide resin, as described previously.[14] Briefly, deprotection of the peptide and cleavage from the resin were achieved by treatment with a trifluoroacetic acid/ethanedithiol mixture (95:5) at room temperature for 3 hours followed by reversed-phase high-performance liquid chromatography purification. Fluorescent labeling at the amino-terminus of the peptides was conducted by treatment with fluorescein isothiocyanate (FITC; Invitrogen, Carlsbad, CA) in a dimethylformamide/methanol mixture (1:1) for 1.5 hours followed by HPLC purification. The structure of the products was confirmed by matrix-assisted laser desorption ionization time-of-flight mass spectrometry. As a control, we synthesized FITC-conjugated 11 poly-glutamate (11E-FITC), which consists of 11 glutamates, acidic amino acids, and FITC. Q2

The structure of each peptide was as follows:

1. FITC-conjugated 11 poly-arginine (11R-FITC):

FITC-RRRRRRRRRRR-COOH

2. 11E-FITC

FITC-EEEEEEEEEEE-COOH.

Animal Studies

All animal procedures were approved by the Animal Ethics Committee of Kurume University and followed the Guide for the Care and Use of Experimental Animals of the university. C57BL/6 male mice, aged 8-9 weeks (20-24 g), were assigned to transient focal cerebral ischemia followed by systemic injection of peptides.

Systemic Injection of Peptides

Mice were anesthetized by inhaling 1.2% concentration of isoflurane in air under spontaneous breathing. 11R-FITC (.2 μmol) or 11E-FITC (.2 μmol) was dissolved in 20-μL saline and then injected into the right femoral vein.

Transient Focal Cerebral Ischemia

Mice were anesthetized by inhaling 1.2% concentration of isoflurane in air under spontaneous breathing. The rectal temperature was controlled at 37.0 ± .5°C via a temperature-regulated heating pad during surgery. Focal cerebral ischemia was induced by occluding the middle cerebral artery (MCA) using the intraluminal filament technique. The right common carotid artery (CCA) was exposed via a midline pretracheal incision. The external carotid artery was ligated. The CCA was then ligated permanently, and a small incision was made 1 mm distal to the ligation. A 6-0 nylon monofilament coated with silicone (Doccol Corporation, Sharon, MA) was introduced through a small incision in CCA and advanced 9 mm distal to the carotid bifurcation. The wound was sutured and the animal returned to its cage. After a 120-minute occlusion period, the mouse was reanesthetized and reperfusion was accomplished by withdrawing the intraluminal filament from the CCA. Immediately after reperfusion, .2 μmol 11R-FITC or .2 μmol 11E-FITC dissolved in 20-μL saline was injected into the right femoral vein.

Assessment of Cerebral Blood Flow

To monitor regional cerebral blood flow continuously, a laser Doppler flowmetry probe was fixed to the intact skull (2 mm posterior and 5 mm lateral to the bregma). Only mice whose regional cerebral blood flow showed a drop of more than 70% from the baseline just after MCAO were included.

Immunohistochemistry

At 1, 2, 4, and 8 hours after peptide injection, mice were deeply anesthetized with an overdose of pentobarbital and perfused transcardially with heparinized physiological saline followed by 4% paraformaldehyde in .1 M phosphate-buffered saline (PBS). The brains and livers were removed, cut into 2-mm coronal sections, fixed in 4% paraformaldehyde in .1 M PBS for 4 hours, and immersed in 30% sucrose in .1 M PBS overnight. Brains were embedded in OCT compound (Tissue-Tek; Sakura Finetek, Tokyo, Japan) and frozen in liquid nitrogen. Q3 Brain and liver sections at a thickness of 10 μm were prepared using a cryostat. The sections were washed 3 times in .1 M PBS and then immersed for 30 minutes in 1% vH_2O_2 and preblocked with .1% Triton X-100 and 1% bovine serum albumin in PBS for 1 hour. The brain sections were then incubated with goat anti-FITC polyclonal antibody (1:200; GeneTex, Irvine, CA) overnight. Excess antibody was washed 4 times by PBS, and then the sections were incubated with biotinylated anti-goat immunoglobulin G (IgG) (H + L) (1:200; Vector Laboratories, Burlingame, CA) for 2 hours. The reaction products were visualized using an ABC kit (Nacalai Tesque, Kyoto, Japan) followed by DAB as a substrate. Q4

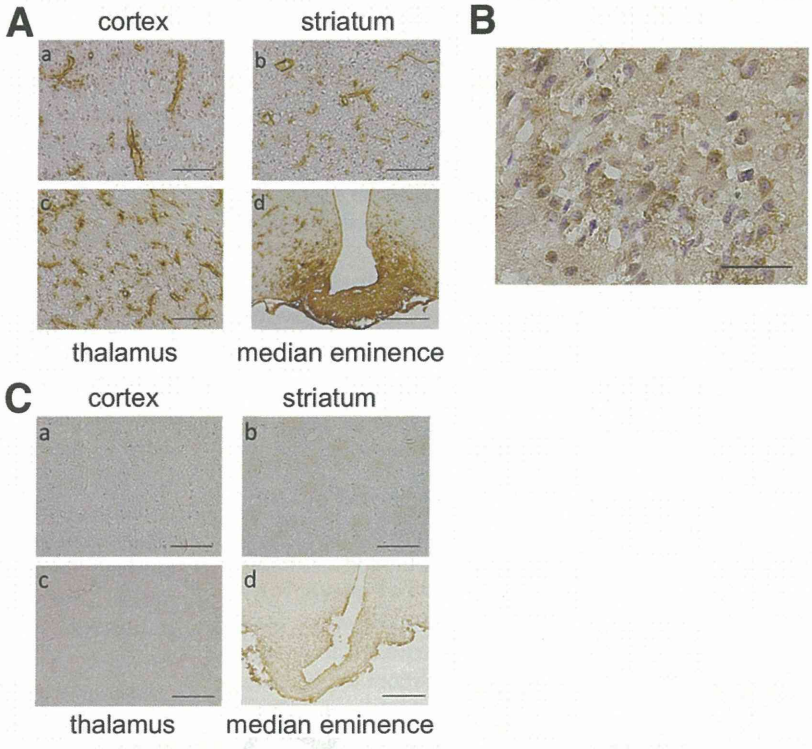

Figure 1. *Transduction of 11R-FITC into the intact mouse brain. (A) At 1 hour after administration of 11R-FITC, FITC signals were detected in the vessels and cells surrounding the vessels of the cortex, striatum, and thalamus. Strong immunoreactivity was detected in the cells of the median eminence. Bars in a, b, and c = 100 μm and d = 200 μm. (B) FITC signals 4 hours after 11R-FITC injection in the striatum. Weak signals were observed in the cells. Bar = 50 μm. (C) Transduction of 11E-FITC. 11E-FITC was systemically administrated to mice. After 4 hours, 11E-FITC was detected by immunohistochemistry using anti-FITC antibody. No FITC signals were observed in cells of the brain. Bars in a, b, and c = 100 μm and d = 200 μm. Abbreviations: FITC, fluorescein isothiocyanate; 11E-FITC, FITC-conjugated 11 poly-glutamate; 11R-FITC, FITC-conjugated 11 poly-arginine.*

For double-labeled immunofluorescence staining, sections were washed 3 times in .1 M PBS and preblocked with .1% Triton X-100 and 1% bovine serum albumin in PBS for 1 hour. The sections were then incubated with goat anti-FITC polyclonal antibody (1:200 dilution; GeneTex) and rabbit anti-NeuN polyclonal antibody (1:100 dilution; Bioss, Wobum, MA), rabbit anti-glial fibrillary acidic protein (GFAP) polyclonal antibody (1:1000 dilution; Imgenex, San Diego, CA) or rabbit anti-ionized calcium-binding adaptor molecule 1 (Iba1) polyclonal antibody (1:1000 dilution; Wako, Osaka, Japan) overnight. Excess antibodies were washed 4 times, and then the sections were incubated with Alexa Fluor488 donkey anti-goat IgG (H + L) (1:200 dilution; Life Technologies, Grand Island, NY) and Alexa Fluor594 donkey anti-rabbit IgG (H + L) (1:200; Invitrogen) for 2 hours. Excess antibody was washed 3 times, and the sections were observed under a confocal microscope (FV-1000; Olympus, Tokyo, Japan).

Optical Density Measurement

Quantification of the optical density (OD) of 11R-FITC immunoreactivity was performed using ImageJ software (National Institutes of Health, MD). The cortex and the striatum were outlined manually, and OD was automatically analyzed on gray-scale images using a computer program. The baseline OD quantified 11R-FITC immunoreactivity in the brain slices of mice without 11R-FITC injection. Previous studies have shown that OD measurements reflect changes in protein expression parallel to those obtained using a biochemical protein assay.[15,16]

Statistical Analyses

Data are shown as the mean (standard error of the mean). Data were analyzed by analysis of variance to compare means between multiple groups followed by post hoc examination, and P less than .05 was considered significant.

Results

Transduction of 11R-FITC into the Normal Brain

To investigate whether 11R is capable of in vivo delivery into the intact brain across the BBB, mice were systemically administrated 11R-FITC. Strong immunoreactivity was observed in the vessels of the cortex, striatum, and thalamus and in the cells surrounding the vessels 1 hour after injection (Fig 1, A). 11R-FITC was also efficiently delivered to the median eminence, where the BBB is not present (Fig 1, A).[17,18] A weak immunoreactive signal was observed in the cells of the cortex, striatum, and thalamus at 4 hours (Fig 1, B) and had almost disappeared throughout all regions in the brain 8 hours after the injection (data not shown). To investigate whether the transduction of 11R-FITC was mediated by the poly-arginine motif, 11E-FITC was systemically administrated into mice. 11E-FITC was not detected in any regions of the brain (Fig 1, C). These results suggest that 11R is capable of in vivo delivery to the

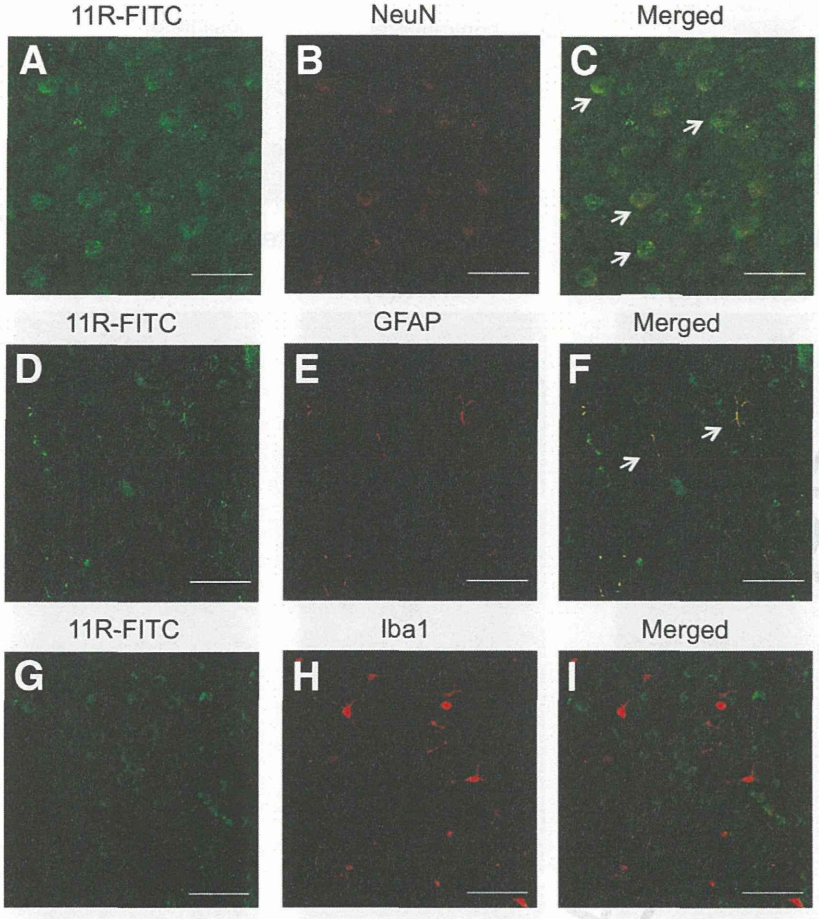

Figure 2. *Transduction of 11R-FITC in neuronal and non-neuronal cells. Mice were systemically administrated with 11R-FITC. After 4 hours, mice were sacrificed and double-immunohistochemical analyses were performed. (A-C) Delivery of 11R-FITC to neurons of the cortex was examined using anti-FITC and anti-NeuN antibodies. Arrows indicate localization of 11R-FITC in NeuN-positive cells. Bars = 50 μm. (D-F) Delivery of 11R-FITC to astrocytes of the striatum was examined using anti-FITC and -GFAP antibodies. Arrows indicate localization of 11R-FITC in GFAP-positive cells. (G-I) Delivery of 11R-FITC to microglia/macrophages of the cortex was examined using anti-FITC and anti-Iba1 antibodies. 11R-FITC was not colocalized with Iba1-positive cells. Bars = 50 μm. Abbreviations: FITC, fluorescein isothiocyanate; GFAP, glial fibrillary acidic protein; Iba-1, ionized calcium-binding adaptor molecule 1; 11R-FITC, FITC-conjugated 11 poly-arginine.*

cells surrounding the vessels across the BBB but cannot deliver extensively to the brain regions.

To observe the amount of 11R-FITC trapped in the liver, we observed the immunoreactivity in the liver after administration of 11R-FITC. Strong immunoreactivity was observed in the liver at 1, 2, 4, and 8 hours after 11R-FITC administration (data not shown), suggesting that a considerable number of peptides were trapped in the liver.

Transduction of 11R-FITC to Neurons

To identify the cells receiving 11R-FITC in the normal brain, mice were systemically administrated 11R-FITC. At 4 hours after injection, the localization of 11R-FITC was examined by immunostaining against a neuronal specific marker, NeuN. As expected, 11R-FITC was efficiently delivered to NeuN-positive neurons (Fig 2, A-C). Notably, 11R-FITC was also colocalized with GFAP, a marker protein of astrocytes in the striatum (Fig 2, D-F), suggesting that 11R could be delivered to both neuronal and non-neuronal cells across the BBB on systemic administration. In contrast, 11R-FITC was not colocalized with Iba1, a microglia/macrophage marker, suggesting that 11R-FITC is delivered in neither microglia nor macrophages (Fig 2, G-I).

Transduction of 11R-FITC into the Ischemic Brain Lesion

On successful delivery of 11R to the intact brain, we next investigated in vivo delivery into an ischemic lesion in the mouse brain (Fig 3, A). We performed MCA occlusion in mice for 2 hours and then systemically administrated 11R-FITC. At 1 hour after injection of 11R-FITC, strong immunoreactivity of 11R-FITC was observed in both contralateral and ipsilateral regions, such as the cortex and striatum of the brain (Fig 3, B); however, the localization of 11R-FITC was apparently different between the 2 regions. In the contralateral region, where the BBB was still intact after ischemia, 11R-FITC was mainly found in cells surrounding vessels, the same as in the normal brain, shown in Figure 1 (Fig 3, B). On the other hand, on the ipsilateral side, where the BBB was opened by transient ischemia, 11R-FITC was intensively delivered to cells of the cortex and striatum in addition to the vessel areas (Fig 3, B). At 2 and 4 hours after injection, strong immunoreactivity of 11R-FITC

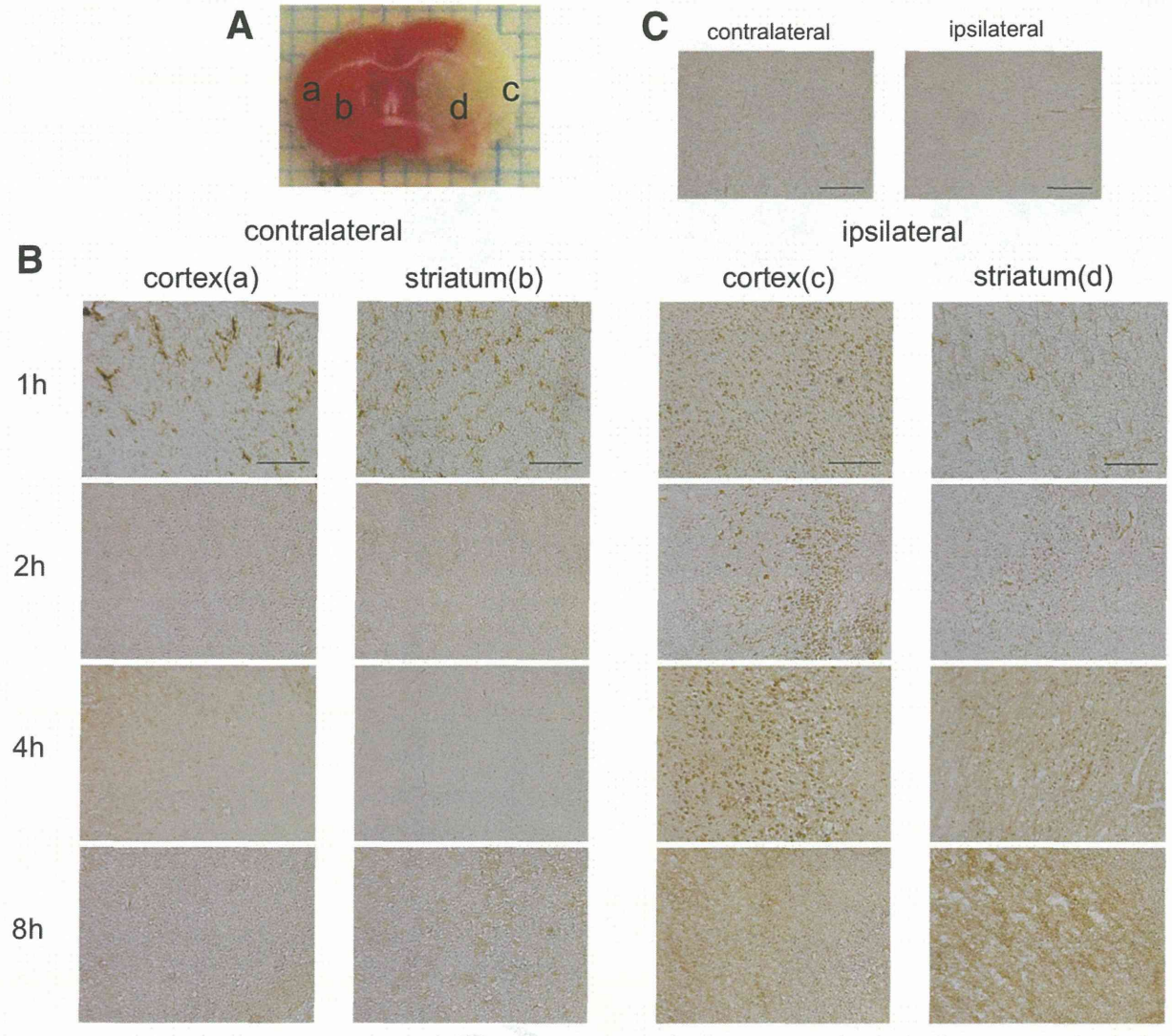

Figure 3. *Transduction of 11R-FITC into an ischemic lesion of the mouse brain. (A) Focal cerebral ischemia was induced by occlusion of middle cerebral artery using the intraluminal filament technique. Areas a and b indicate the cortex and striatum on the contralateral side, respectively. Areas c and d indicate the cortex and striatum on the ipsilateral side, respectively. (B) Localization of 11R-FITC in the cortex and striatum of contralateral and ipsilateral sides was examined 1, 2, 4, and 8 hours after systemic administration. a and b, cortex and striatum on the contralateral side; c and d, cortex and striatum on the ipsilateral side. Bars = 200 μm. (C) After transient ischemic injury, mice were systemically administrated 11E-FITC. Four hours after injection, 11E-FITC in the cortex was examined by immunostaining. Bars = 200 μm. Abbreviations: FITC, fluorescein isothiocyanate; 11E-FITC, FITC-conjugated 11 poly-glutamate; 11R-FITC, FITC-conjugated 11 poly-arginine.*

was observed in cells in the ipsilateral region, whereas 11R-FITC was faint on the contralateral side. Even at 8 hours after injection, 11R-FITC was still detectable on the ipsilateral side with some leakage of 11R-FITC to the interstitium. In contrast, 11R-FITC had disappeared on the contralateral side 8 hours after injection (Fig 3, B). To investigate whether 11R-FITC selectively crosses the BBB in a CPP-dependent manner or just diffuses through altered BBB during ischemic injury on the ipsilateral side, 11E-FITC was systemically administrated after transient ischemia. 11E-FITC was not detected in either contralateral or ipsilateral regions of the brain (Fig 3, C).

To confirm that 11R-FITC was not delivered into microglia/macrophages activated by ischemia, double-labeled immunofluorescence staining was performed with anti-Iba1 and anti-FITC antibodies in the ischemic region. 11R-FITC was not colocalized with Iba1 at 4 hours after injection (Fig 4).

The kinetics of peptide transduction during ischemia was examined by measuring the optic density of 11R-FITC in cortex and striatum at each time point after the administration (Fig 5, A,B). In both the cortex and striatum, immunoreactivity of 11R-FITC on the ipsilateral side was significantly higher than on the contralateral side (P = .0043 in cortex and P = .0031 in striatum).

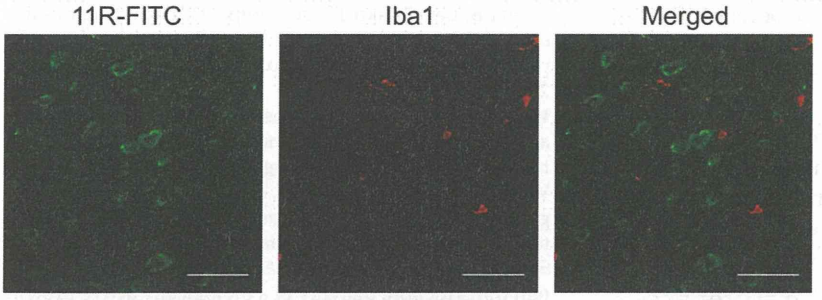

Figure 4. *Double-labeled immunofluorescence staining after ischemic injury. In an ischemic lesion of the brain, delivery of 11R-FITC to microglia/macrophages 4 hours after ischemic injury was examined using anti-FITC and anti-Iba1 antibodies. 11R-FITC was not colocalized with Iba1-positive cells. Bars = 50 μm. Abbreviations: FITC, fluorescein isothiocyanate; Iba-1, ionized calcium-binding adaptor molecule 1; 11R-FITC, FITC-conjugated 11 poly-arginine.*

Although the time effect was not significant, on the ipsilateral side, 11R-FITC was at its highest 1 hour after injection in the cortex and remained detectable in the cortex and striatum for 8 hours after administration.

Discussion

In the present study, we aimed to investigate whether 11R could cross the BBB and reach cells in a normal brain or with an ischemic injury. In the intact brain, 11R-FITC was observed throughout the brain, including the cortex, striatum, and thalamus. Although 11R was highly localized in vessels, it was also detected in both neuronal and non-neuronal cells in the peripheral brain area surrounding vessels. These results suggest that 11R is capable of crossing the BBB and being delivered into the brain; however, the delivery efficiency of 11R in the intact brain is relative low when compared with that in non-neuronal regions.[13,19] The low efficiency of peptide delivery by 11R may be because of the unique biological properties of BBB and the pharmacokinetic properties of 11R. To prevent leakage of harmful molecules into the nervous system, the endothelial cells in the BBB are cemented together by tight junctions and have reduced macropinocytosis.[20] Because CPP-mediated delivery is mainly through macropinocytosis,[8] uptake of 11R would be, thus, inevitably attenuated in an intact BBB. In addition, a large amount of 11R may be metabolized by BBB-specific drug efflux transporters or peptidases.[21] On the other hand, the low transduction efficiency of 11R could also be because of a decrease in the net amount of circulating 11R because we detected a considerable amount of 11R-FITC peptides trapped in the liver after systemic administration (data not shown). Nevertheless, the current results suggest that 11R-mediated delivery is a reliable tool for brain delivery compared with the controversial TAT-mediated delivery.

It is generally accepted that the molecular weight of molecules transported into the brain through the BBB is less than 400-600 Da.[22-24] In the present study, however, 11R-FITC, with a molecular weight of 2239 Da, could be delivered into the brain. Moreover, a previous study showed that TAT-derived PTD was capable of transducing β-galactosidase, which has a molecular weight of more than 100 kDa, into the brain. These results suggest that there may be no limit to the molecular weight of molecules transduced by CPP. Further study of the size dependency of protein delivery into the brain using 11R is required.

11R-mediated delivery was greatly enhanced in the ischemic model up to 8 hours after systemic administration. Interestingly, 11R was not detected in large vessels on the ischemic side compared with the dense localization of 11R on the contralateral side. This may be caused by reduced cerebral blood flow on the ischemic side of the brain by microcirculatory disturbances and occlusion of CCA.[25] The precise mechanism by which delivery of 11R was enhanced on the ischemic side is unclear. It is

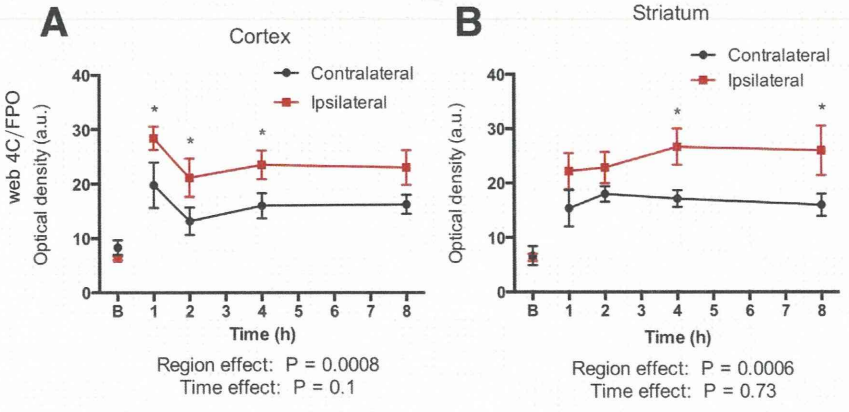

Figure 5. *Statistical analysis of transduction of 11 poly-arginine (11R) in the cortex and striatum after ischemic injury. Optical density (OD) of fluorescein isothiocyanate–conjugated 11R was measured at each time point shown in Figure 3,B. Significance was examined by 2-way analysis of variance. *P < .05. "B" means the baseline OD; n = 4-6.*

known that, in disease states, the BBB becomes less restrictive to proteins or cells by enhanced transcytosis through altered tight junctions.[20] Such leakage of the BBB could continue for up to several weeks following temporary focal ischemia.[26] The enhanced uptake of 11R could be caused by a leaky BBB during transient ischemic injury; however, given the finding that poly-glutamate (11E) did not cross the BBB at all, it is unlikely that 11R crossed the BBB through a nonspecific diffusion model. Rather, 11R was delivered through a highly regulated CPP-dependent manner in the ischemic brain.

In addition to the biological properties, the pathogenicity of PTD-mediated delivery needs to be taken into consideration for therapeutic utilization. Thus, consideration is particularly important when using virus-derived PTD such as TAT. Indeed, TAT has been shown to impair neuronal activity and learning and memory.[27-29] Therefore, although some groups have used TAT to deliver proteins into an intact brain or ischemic regions of the brain,[9,10,30] it is conceivable that TAT might cause unexpected side effects in the brain. In contrast to TAT, 11R is a synthetic peptide and has not been associated with any pathogenesis during in vivo administration.[13]

Taken together, our results suggest that 11R may be used as a potential tool to deliver therapeutic molecules to the brain for the treatment of ischemia.

Conclusions

In this study, we demonstrated that 11R could be delivered to the intact brain across the BBB on systemic administration. Furthermore, the delivery was remarked enhanced and continued up to 8 hours in the brain area affected by transient ischemic injury, suggesting the potential therapeutic application of 11R-mediated delivery.

Acknowledgment: This work was supported by a Grant-in-aid for Scientific Research from the Ministry of Education, Culture, Sports, Science and Technology of Japan and by the Japan Society for the Promotion of Science (JSPS) through its "Funding Program for Next Generation World-Leading Researchers."

References

1. Kelly-Hayes P, Robertson J, Broderick J, et al. The American Heart Association stroke outcome classification. Stroke 1998;29:1274-1280.
2. Taqi MA, Vora N, Callison RC, et al. Past, present, and future of endovascular stroke therapies. Neurology 2012;79:S213-S220.
3. de Lange EC. The physiological characteristics and transcytosis mechanisms of the blood-brain barrier (BBB). Curr Pharm Biotechnol 2012;13:2319-2327.
4. Pardridge WM. Blood-brain barrier delivery of protein and non-viral gene therapeutics with molecular Trojan horses. J Control Release 2007;122:345-348.
5. Joliot A, Prochiantz A. Transduction peptides: from technology to physiology. Nat Cell Biol 2004;6:189-196.
6. Gupta B, Levchenko TS, Torchilin VP. Intracellular delivery of large molecules and small particles by cell-penetrating proteins and peptides. Adv Drug Deliv Rev 2005;57:637-651.
7. Wadia JS, Dowdy SF. Transmembrane delivery of protein and peptide drugs by TAT-mediated transduction in the treatment of cancer. Adv Drug Deliv Rev 2005;57:579-596.
8. Wadia JS, Stan RV, Dowdy SF. Transducible TAT-HA fusogenic peptide enhances escape of TAT-fusion proteins after lipid raft macropinocytosis. Nat Med 2004;10:310-315.
9. Schwarze SR, Ho A, Vocero-Akbani A, et al. In vivo protein transduction: delivery of a biologically active protein into the mouse. Science 1999;285:1569-1572.
10. Cao G, Pei W, Ge H, et al. In vivo delivery of a Bcl-xL fusion protein containing the TAT protein transduction domain protects against ischemic brain injury and neuronal apoptosis. J Neurosci 2002;22:5423-5431.
11. Fawell S, Seery J, Daikh Y, et al. Tat-mediated delivery of heterologous proteins into cells. Proc Natl Acad Sci U S A 1994;91:664-668.
12. Simon MJ, Kang WH, Gao S, et al. TAT is not capable of transcellular delivery across an intact endothelial monolayer in vitro. Ann Biomed Eng 2011;39:394-401.
13. Noguchi H, Matsushita M, Okitsu T, et al. A new cell-permeable peptide allows successful allogeneic islet transplantation in mice. Nat Med 2004;10:305-309.
14. Takayama K, Nakase I, Michiue H, et al. Enhanced intracellular delivery using arginine-rich peptides by the addition of penetration accelerating sequences (Pas). J Control Release 2009;138:128-133.
15. Mufson EJ, Lavine N, Jaffar S, et al. Reduction in p140-TrkA receptor protein within the nucleus basalis and cortex in Alzheimer's disease. Exp Neurol 1997;146:91-103.
16. Moeller ML, Dimitrijevich SD. A new strategy for analysis of phenotype marker antigens in hollow neurospheres. J Neurosci Methods 2004;139:43-50.
17. Noda M. The subfornical organ, a specialized sodium channel, and the sensing of sodium levels in the brain. Neuroscientist 2006;12:80-91.
18. Sisó S, Jeffrey M, González L. Sensory circumventricular organs in health and disease. Acta Neuropathol 2010; 120:689-705.
19. Matsui H, Tomizawa K, Lu YF, et al. Protein therapy: in vivo protein transduction by polyarginine (11R) PTD and subcellular targeting delivery. Curr Protein Pept Sci 2003;4:151-157.
20. Banks WA. Characteristics of compounds that cross the blood-brain barrier. BMC Neurol 2009;9(Suppl 1):S3.
21. Candelario-Jalil E, Yang Y, Rosenberg GA. Diverse roles of matrix metalloproteinases and tissue inhibitors of metalloproteinases in neuroinflammation and cerebral ischemia. Neuroscience 2009;158:983-994.
22. Pardridge WM. The blood-brain barrier: bottleneck in brain drug development. NeuroRX 2005;2:3-14.
23. Cardoso FL, Brites D, Brito MA. Looking at the blood-brain barrier: molecular anatomy and possible investigation approaches. Brain Res Rev 2010;64:328-363.
24. Kilic U, Kilic E, Dietz GP, et al. Intravenous TAT-GDNF is protective after focal cerebral ischemia in mice. Stroke 2003;34:1304-1310.
25. Lu H, Zhao J, Li M, et al. Microvessel changes after post-ischemic benign and malignant hyperemia: experimental study in rats. BMC Neurol 2010;10:24.
26. Strbian D, Durukan A, Pitkonen M, et al. The blood-brain barrier is continuously open for several weeks following transient focal cerebral ischemia. Neuroscience 2008; 153:175-181.

27. Li ST, Matsushita M, Moriwaki A, et al. HIV-1 Tat inhibits long-term potentiation and attenuates spatial learning. Ann Neurol 2004;55:362-371.
28. Carey AN, Sypek EI, Singh HD, et al. Expression of HIV-Tat protein is associated with learning and memory deficits in the mouse. Behav Brain Res 2012;229: 48-56.
29. Kim HJ, Martemyanov KA, Thayer SA. Human immunodeficiency virus protein Tat induces synapse loss via a reversible process that is distinct from cell death. J Neurosci 2008;28:12604-12613.
30. Cai B, Lin Y, Xue XH, et al. TAT-mediated delivery of neuroglobin protects against focal cerebral ischemia in mice. Exp Neurol 2011;227:224-231.